Original Article | Neuroimaging and Head & Neck

eISSN 2005-8330
https://doi.org/10.3348/kjr.2022.0850
Korean J Radiol 2023;24(9):860-870

Korean Journal of Radiology
KJR

Imaging of Facial Nerve With 3D-DESS-WE-MRI Before Parotidectomy: Impact on Surgical Outcomes

Han-Sin Jeong[1], Yikyung Kim[2], Hyung-Jin Kim[2], Hak Jung Kim[1], Eun-hye Kim[1], Sook-young Woo[3], Man Ki Chung[1], Young-Ik Son[1]

[1]Department of Otorhinolaryngology-Head and Neck Surgery, Samsung Medical Center, Sungkyunkwan University School of Medicine, Seoul, Republic of Korea
[2]Department of Radiology, Samsung Medical Center, Sungkyunkwan University School of Medicine, Seoul, Republic of Korea
[3]Center for Biomedical Statistics, Samsung Medical Center, Seoul, Republic of Korea

Objective: The intra-parotid facial nerve (FN) can be visualized using three-dimensional double-echo steady-state water-excitation sequence magnetic resonance imaging (3D-DESS-WE-MRI). However, the clinical impact of FN imaging using 3D-DESS-WE-MRI before parotidectomy has not yet been explored. We compared the clinical outcomes of parotidectomy in patients with and without preoperative 3D-DESS-WE-MRI.

Materials and Methods: This prospective, non-randomized, single-institution study included 296 adult patients who underwent parotidectomy for parotid tumors, excluding superficial and mobile tumors. Preoperative evaluation with 3D-DESS-WE-MRI was performed in 122 patients, and not performed in 174 patients. FN visibility and tumor location relative to FN on 3D-DESS-WE-MRI were evaluated in 120 patients. Rates of FN palsy (FNP) and operation times were compared between patients with and without 3D-DESS-WE-MRI; propensity score matching (PSM) and inverse probability of treatment weighting (IPTW) were used to adjust for surgical and tumor factors.

Results: The main trunk, temporofacial branch, and cervicofacial branch of the intra-parotid FN were identified using 3D-DESS-WE-MRI in approximately 97.5% (117/120), 44.2% (53/120), and 25.0% (30/120) of cases, respectively. The tumor location relative to FN, as assessed on magnetic resonance imaging, concurred with surgical findings in 90.8% (109/120) of cases. Rates of temporary and permanent FNP did not vary between patients with and without 3D-DESS-WE-MRI according to PSM (odds ratio, 2.29 [95% confidence interval {CI} 0.64–8.25] and 2.02 [95% CI: 0.32–12.90], respectively) and IPTW (odds ratio, 1.76 [95% CI: 0.19–16.75] and 1.94 [95% CI: 0.20–18.49], respectively). Conversely, operation time for surgical identification of FN was significantly shorter with 3D-DESS-WE-MRI (median, 25 vs. 35 min for PSM and 25 vs. 30 min for IPTW, $P < 0.001$).

Conclusion: Preoperative FN imaging with 3D-DESS-WE-MRI facilitated anatomical identification of FN and its relationship to the tumor during parotidectomy. This modality reduced operation time for FN identification, but did not significantly affect postoperative FNP rates.

Keywords: Parotid neoplasms; Facial nerve; Prospective studies; Magnetic resonance imaging; Propensity score

INTRODUCTION

Surgical resection is the primary treatment for parotid gland tumors; however, risk of facial nerve (FN) palsy is a concerning complication [1–5]. For small and superficial tumors, the incidence of FN palsy (FNP) is < 5% [6,7]. However, in large, deep-seated, and malignant tumors, it is > 30% [6–8]. In addition, revision parotidectomy and wide extent of surgery are well-known risk factors for FNP [2,3,9–11].

Several measures have been adopted to prevent FN injury during a parotidectomy. Antegrade dissection of the intra-

Received: September 4, 2022 **Revised:** April 12, 2023 **Accepted:** May 30, 2023
Corresponding author: Yikyung Kim, MD, PhD, Department of Radiology, Samsung Medical Center, Sungkyunkwan University School of Medicine, 81 Irwon-ro, Gangnam-gu, Seoul 06351, Republic of Korea
• E-mail: yk2009.kim@gmail.com

Korean Journal of Radiology
KJR

parotid FN using surgical landmarks is a common approach [12,13]. Intraoperative FN monitoring is an essential tool for identifying and preserving the intra-parotid FN [14–18].

Magnetic resonance imaging (MRI) with a particular sequence, including a three-dimensional double-echo steady state water-excitation (3D-DESS-WE) sequence, has been used to directly visualize the intra-parotid FN [19-25]. Previous studies have reported that 3D-DESS-WE-MRI can more successfully predict the FN-tumor anatomical relationship than conventional indirect prediction methods [26,27].

In addition to the improved imaging ability for the FN using 3D-DESS-WE-MRI, the clinical impact of FN imaging using MRI before parotidectomy remains to be explored. We hypothesized that preoperative FN imaging with 3D-DESS-WE-MRI reduces postoperative FN weakness associated with parotidectomy. This is because it provides an accurate depiction of the FN-tumor relationship, allowing for optimal surgical planning. Thus, this prospective study was conducted to compare surgical outcomes of parotidectomy between patients with and without preoperative FN imaging using 3D-DESS-WE-MRI, and to investigate its clinical impact.

MATERIALS AND METHODS

Study Design

This prospective, non-randomized study compared surgical outcomes of parotidectomy for benign and malignant tumors between patients with and without preoperative FN imaging using 3D-DESS-WE-MRI. The study protocol was approved by the Institutional Review Board of Samsung Medical Center prior to patient enrollment (SMC-IRB-No. 2017-07-084-003) and registered in the clinical trial registry (ClinicalTrials.gov-ID-NCT03822728). All study subjects completed a written informed consent form.

Inclusion, Exclusion, and Patient Allocation

Patients with parotid gland tumors were initially evaluated via cytology, core-needle biopsy, and computed tomography (CT). Surgical cases were screened for enrollment in this study (n = 420) (Fig. 1). Patients older than 18 years who could tolerate surgery and anesthesia were included. We excluded patients with no clear need for FN identification or dissection during parotidectomy (superficial and mobile tumors < 2 cm in diameter on diagnostic imaging and palpation), and those who underwent extracapsular dissection of tumors without identification of the FN main trunk (n = 124).

Based on the potential increased risk of FNP in parotidectomy, 3D-DESS-WE-MRI was performed. This procedure was more likely to be prescribed in complex cases with multiple risk factors; therefore, it was performed for large tumors (≥ 2 cm diameter on CT scans), tumors located medially to a line parallel to the lateral edge of the retromandibular vein on axial CT images, tumors suspicious of malignancy (by cytology or biopsy), and cases for revision surgery [7]. However, the final decision was made considering clinical factors and the surgeon's experience. Consequently, 174 patients did not undergo 3D-DESS-WE-MRI (referred to as the MRI [-] group), and 122 patients underwent 3D-DESS-WE-MRI (referred to as the MRI [+] group). The MRI (-) group did not undergo any MRI imaging of the head and neck region, including 3D-DESS-WE-MRI.

To evaluate surgical outcomes of parotidectomy, cases where the FN was intentionally sacrificed for oncological safety (n = 26) were excluded. Therefore, for outcome analysis, we only included patients managed with the intention of preserving FN function, resulting in 165 patients in the MRI (-) group and 105 patients in the MRI (+) group (Fig. 1).

Imaging Techniques and Surgical Procedures (Parotidectomy)

MRI techniques were similar to those described previously [27]. The details are described in the Supplementary Methods section.

Anatomical Visibility of 3D-DESS-WE-MRI

The tumor location relative to the entire range of the visible FN was determined on 3D-DESS-WE-MRI images (Fig. 2). All magnetic resonance (MR) scans were anonymized and randomly evaluated by two independent neuroradiologists. Any disagreement in MR evaluation was resolved by a consensus with joint interpretation.

First, we evaluated visibility of the main trunk, temporofacial division, and cervicofacial division of the intra-parotid FN on the affected side, as well as inter-observer agreement. Tumors were divided into three subgroups: superficial lobe tumors, located entirely lateral to the FN, deep-lobe tumors, located entirely medial to the FN, and both-lobe tumors, spanning both medial and lateral areas. The anatomical location between the tumor and main trunk of the FN on 3D-DESS-WE-MRI images was evaluated and compared with surgical findings (Fig. 3).

 https://doi.org/10.3348/kjr.2022.0850

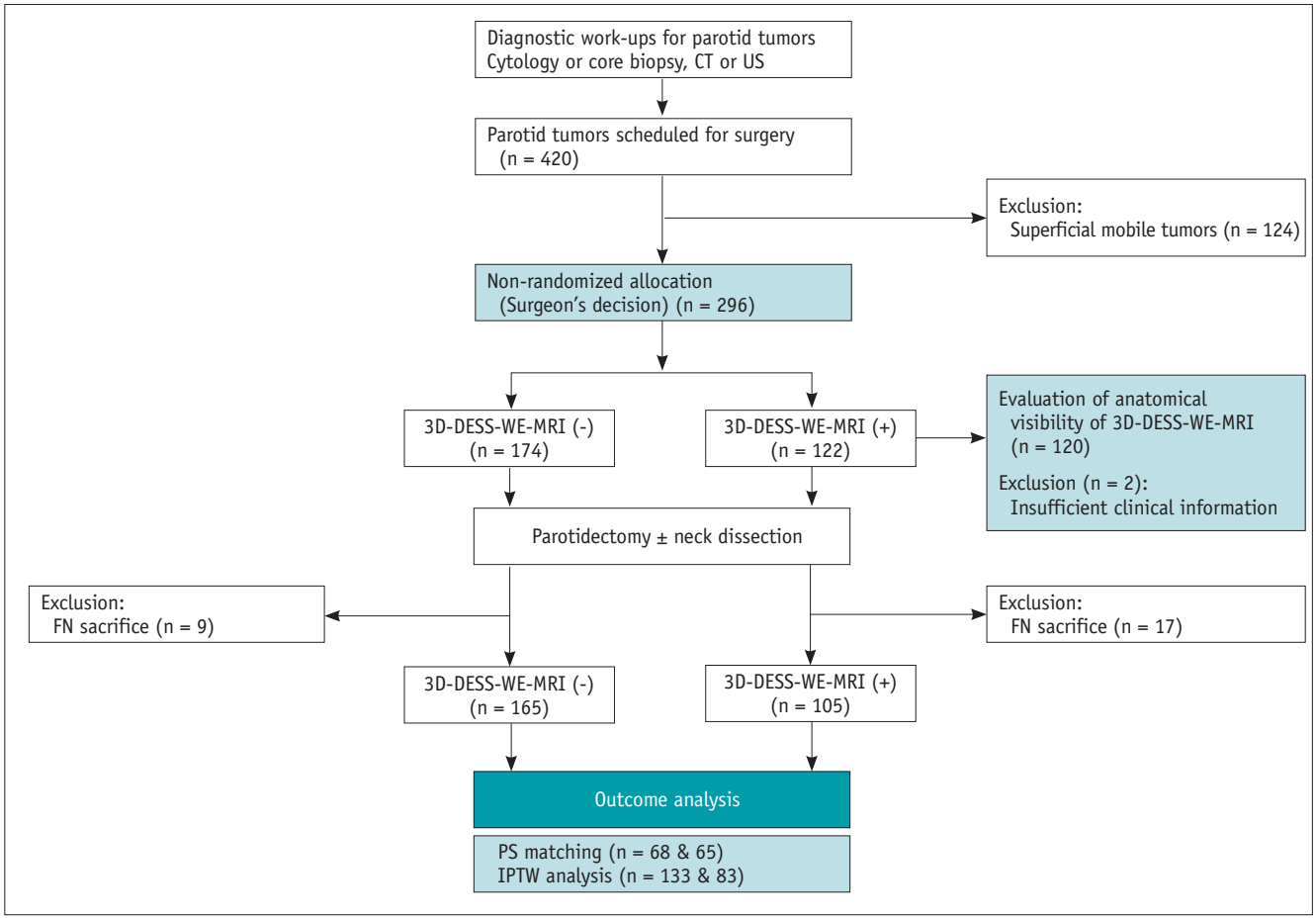

Fig. 1. Study flow diagram. CT = computed tomography, US = ultrasonography, 3D-DESS-WE-MRI = three-dimensional double-echo steady-state water-excitation sequence magnetic resonance imaging, FN = facial nerve, PS = propensity score, IPTW = inverse probability of treatment weighting

Surgical and Tumor Variables for Analyses

Baseline clinical factors of patients were sex and age at the time of surgery. Surgical factors included the surgeon, extent of surgery, and whether revision parotid surgery was performed. Tumor factors included tumor size, multiplicity, location, and pathology according to surgical or pathological results. The details are described in the Supplementary Methods section.

Outcome Measurement

We evaluated the operation time for each surgery to indirectly investigate the assistive role of 3D-DESS-WE-MRI, focusing on two specific times (Supplementary Fig. 1). The first was the time required for FN identification, measured from the end of flap elevation to FN identification of the main trunk (or temporofacial or cervicofacial branches in some partial parotidectomy cases). The second was the time for FN dissection and parotid tumor removal, which was the duration from FN identification to the end of FN dissection and final tumor removal from the parotid bed.

Regarding FN outcomes, FNP incidence was categorized as temporary or permanent. None of the enrolled patients manifested preoperative FN weakness. Postoperatively, any weakness in ipsilateral facial motion (forehead wrinkling, eye closure, nasolabial fold, and lip motion) was recorded and considered temporary FNP. Follow-ups for benign tumors were performed at 3 and 12 months postoperatively, and those for malignant tumors were conducted every 3–6 months for 5 years. FNP persisting for approximately 12 months was regarded as permanent FNP.

Statistical Analyses

For deep-seated parotid tumors, FN weakness has been reported in approximately 10.3%–25.6% of patients after parotidectomy [7]. Thus, we hypothesized that incidence would decrease from 25.0% to 10.0% with preoperative

https://doi.org/10.3348/kjr.2022.0850

Korean Journal of Radiology
KJR

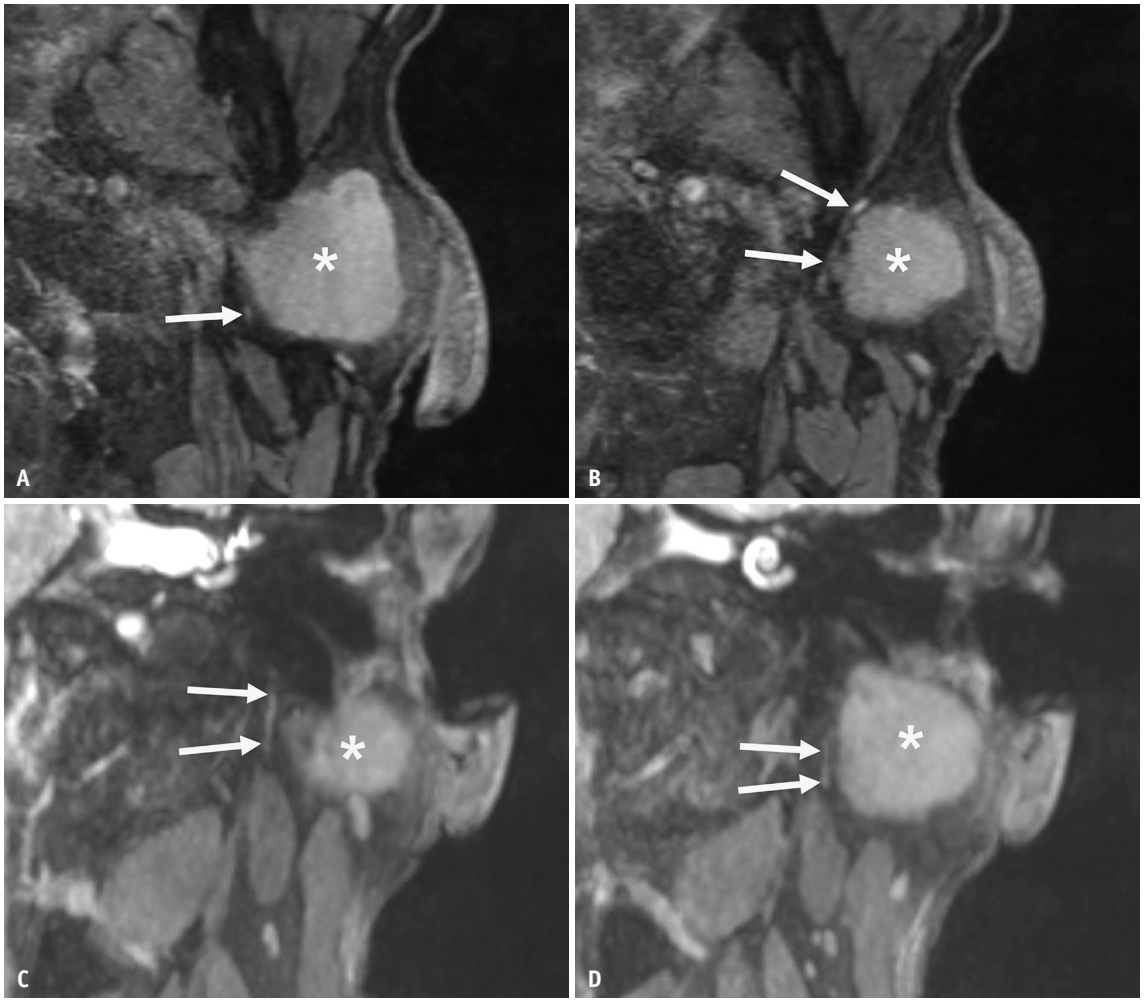

Fig. 2. Representative images of 3D-DESS-WE-MRI in a case with a left parotid gland tumor (pleomorphic adenoma). **A, B:** Serial axial scans. **C, D:** coronal scans. The arrows indicate the main trunk **(A, C)** or the cervicofacial branch **(B, D)** of the intra-parotid facial nerve. Asterisks indicate tumor. 3D-DESS-WE-MRI = three-dimensional double-echo steady-state water-excitation sequence magnetic resonance imaging

FN imaging (MRI) during parotidectomy. This calculation yielded 100 cases per group (1:1 ratio) with an alpha error of 0.05 and a statistical power of 80.0%. Considering dropout rates, we enrolled a minimum of 120 patients in each group.

Continuous variables were compared using Student's *t*-test or Wilcoxon's rank sum test. Categorical variables were compared using Pearson's chi-square test or Fisher's exact test. Inter-observer agreement on detectability of the intra-parotid FN between two observers was calculated using kappa (κ) statistics.

A multivariable logistic regression model was used to obtain propensity scores (PSs) for each participant. Patient grouping (with or without 3D-DESS-WE-MRI) was used as the dependent variable in PS modeling. There were eight independent variables: host factors (age and sex), surgical factors (surgeons and revision surgery), and tumor factors (size, multiplicity, tumor location, and pathology). Surgical extent was not included as an independent variable in the analysis (multicollinearity), as it could be affected by other tumor factors (tumor size, location, or malignancy). Furthermore, clinical findings such as tumor fixation or mobility were highly dependent on tumor size and location; therefore, these variables were excluded from the adjusted matching model. Additionally, we adjusted for the potential mediator effect of surgical extent, to estimate the relative impact of intervention (3D-DESS-WE-MRI) on operation time and FN outcomes. PS was used to produce a 1:1 matching cohort. The nearest-neighbor matching algorithm without replacement was considered using a caliper 0.1 with a standard deviation of the logit of PS. After all PS matching, differences in variables between the two groups were compared by

 https://doi.org/10.3348/kjr.2022.0850

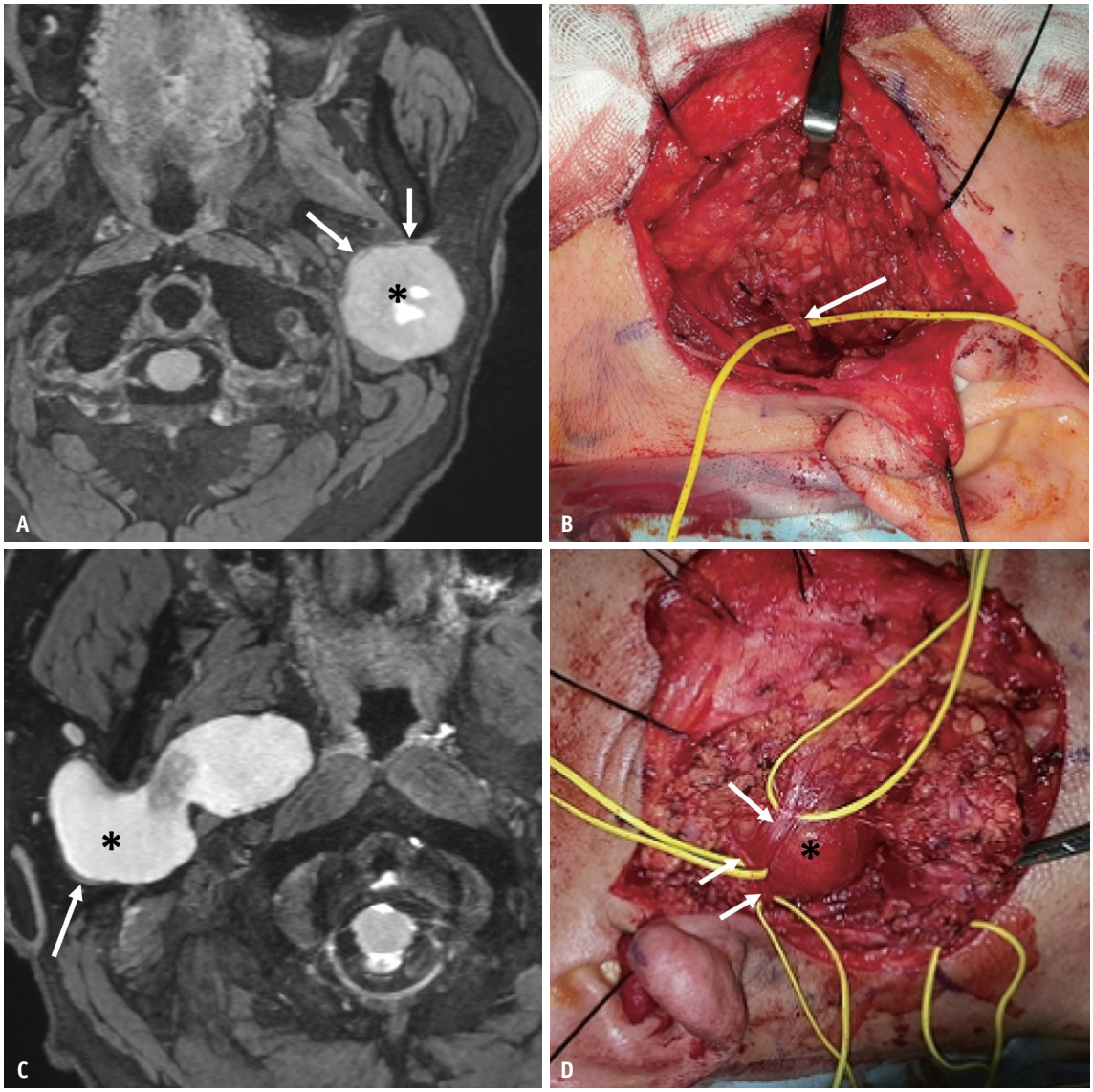

Fig. 3. Comparison of 3D-DESS-WE-MRI images and surgical findings. **A, B:** Superficial-lobe tumor. The left parotid gland tumor (asterisk) is located lateral to the facial nerve (arrows), indicating a superficial-lobe tumor. An intraoperative photograph **(B)** taken after tumor removal demonstrates the facial nerve (arrow) located deep to the tumor. **C, D:** Deep-lobe tumor. The tumor in the right parotid gland (asterisk) is located medial to the facial nerve (arrow), indicating a deep-lobe tumor. An intraoperative photograph **(D)** clearly demonstrates the tumor (asterisk) located deep to the facial nerve (arrows). 3D-DESS-WE-MRI = three-dimensional double-echo steady-state water-excitation sequence magnetic resonance imaging

standardized mean differences, and values ≥ 0.1 were defined as a meaningful imbalance [28,29]. To reduce the influence of possible confounding variables, we used inverse probability of treatment weighting (IPTW) in addition to PS-matched analysis. Stabilized weights were estimated to reduce the weights of either treated participants with low PS or untreated participants with high PS. Weights were trimmed to the lower 10% and upper 90% [30-32].

In the PS-matched cohort, outcomes between groups were compared using regression analyses, including logistic regression with generalized estimating equations [33]. The outcomes were operation time (time to FN identification and time to tumor removal) and rate of FNP (temporary or permanent). Statistical significance was set at a two-sided *P*-value of < 0.05. Data analyses were conducted using R 4.0.4 (The R Foundation; https://www.R-project.org/).

RESULTS

Patient Characteristics and Risk Factors for FNP

Clinical and tumor characteristics of the overall study group and MRI (+) and MRI (-) groups are summarized in

https://doi.org/10.3348/kjr.2022.0850

Korean Journal of Radiology
KJR

Table 1. Clinical and tumor characteristics of enrolled patients

Variables	Before PS matching				After PS matching			
	MRI (-) (n = 165)	MRI (+) (n = 105)	*P*	SMD	MRI (-) (n = 65)	MRI (+) (n = 65)	*P*	SMD
Age, yr	51.4 ± 13.9	47.4 ± 13.4	0.034*	-0.26	49.0 ± 14.5	46.9 ± 15.3	0.429*	-0.13
Sex								
Male	89 (53.9)	35 (33.3)	0.001	-0.44	25 (38.5)	27 (41.5)	0.858	0.07
Female	76 (46.1)	70 (66.7)			40 (61.5)	38 (58.5)		
Surgical factors								
Surgeons								
Surgeon #1	99 (60.0)	93 (88.6)	< 0.001	0.9	56 (86.2)	55 (84.6)	> 0.999	-0.05
Surgeon #2–3	66 (40.0)	12 (11.4)			9 (13.8)	10 (15.4)		
Revision surgery								
Yes	5 (3.0)	3 (2.9)	> 0.999†	-0.01	3 (4.6)	2 (3.1)	> 0.999†	-0.09
Tumor factors								
Size, median (IQR), cm	2.7 (2.3 to 3.5)	3.5 (2.9 to 4.0)	< 0.001‡	0.43	3.0 (2.3 to 4.0)	3.1 (2.7 to 3.6)	0.212‡	0.07
Multiplicity								
Yes	7 (4.2)	5 (4.8)	> 0.999†	0.02	4 (6.2)	2 (3.1)	0.680†	-0.14
Tumor location								
Superficial lobe	133 (80.6)	54 (51.4)	< 0.001	-0.59	42 (64.6)	42 (64.6)	1.000	< 0.01
Deep or both lobe	32 (19.4)	51 (48.6)			23 (35.4)	23 (35.4)		
Pathology								
Benign	144 (87.3)	77 (73.3)	0.006	0.32	51 (78.5)	55 (84.6)	0.498	-0.14
Malignancy	21 (12.7)	28 (26.7)			14 (21.5)	10 (15.4)		

Values are presented as mean ± standard deviation or n (%) unless otherwise indicated. Surgeon factor: Surgeon #1: parotid surgery > 100/year, surgical experience in the head and neck field = 20 years, Surgeon #2: parotid surgery = 20–30/year, surgical experience in the head and neck field = 25 years, Surgeon #3: parotid surgery = 20–30/year, surgical experience in the head and neck field = 15 years. Temporary FNP: < 6 months after parotidectomy, Permanent FNP: persistent FNP at 6–18 months after parotidectomy. Operation time: See Supplementary Fig. 1. Statistical tests without symbols used Pearson's Chi-squared test.
*Student T-test, †Fisher's exact test for count data, ‡Wilcoxon's rank-sum test.
PS = propensity score, MRI = magnetic resonance imaging, SMD = standardized mean difference, IQR = interquartile range, FNP = facial nerve palsy

Table 1. The main parotid surgeon (#1) prescribed more 3D-DESS-WE-MRI for parotid tumor patients. Tumors in the MRI (+) group were larger in size, deeper in location, more malignant, and had a wider surgical extent (parotidectomy). Therefore, unadjusted apparent incidences of temporary and permanent FNP were higher in the MRI (+) group (24.8% and 15.2%, respectively) than in the MRI (+) group (2.4% and 1.2%, respectively).

To compare our findings with those of previous reports, we reviewed incidence of FNP in the entire patient group (with and without MRI intervention) (Supplementary Table 1). As expected, tumor factors such as tumor size ($P = 0.008$, temporary FNP), tumor location ($P = 0.001$, temporary FNP; $P = 0.014$, permanent FNP), and pathology (malignant tumors) ($P < 0.001$, temporary FNP; $P < 0.0001$, permanent FNP) were significant risk factors for FNP. Additionally, 3D-DESS-WE-MRI was a significant factor for FNP in multivariable analyses ($P = 0.002$, temporary FNP; $P = 0.01$, permanent FNP) (Supplementary Table 2).

Anatomical Visibility of 3D-DESS-WE-MRI

In patients with preoperative 3D-DESS-WE-MRI, excluding two cases without adequate surgical descriptions (n = 120), we evaluated the MRI depiction of FN and tumor location. According to the consensus interpretation, preoperative FN imaging identified the main trunk and temporofacial and cervicofacial branches of the intra-parotid FN in 97.5% (117/120), 44.2% (53/120), and 25.0% (30/120) of cases, respectively. Inter-observer agreement was excellent for detection of the main trunk ($\kappa = 1$) and good for detection of the temporofacial ($\kappa = 0.79$) and cervicofacial ($\kappa = 0.70$) divisions.

Surgical findings revealed 57 superficial-lobe, 18 deep-lobe, and 45 both-lobe tumors. Concordance of the tumor location relative to the FN as assessed on 3D-DESS-WE-MRI with the surgical findings was 90.8% (109/120) (Table 2).

 https://doi.org/10.3348/kjr.2022.0850

Impact of Preoperative FN Imaging on the Operation Time and FNP

PS matching and IPTW were used to adjust for unequal distribution of risk factors for FNP in the two groups. PS matching methods resulted in relatively well-adjusted comparison groups, as confirmed by paired histograms and love plots (Supplementary Fig. 2). PS matching resulted in 65 patients in both groups (Table 1, Supplementary Table 3). Consequently, the standardized mean differences of matching variables were < 0.15 (Table 1, Supplementary Table 4). The stabilized IPTW model led to a pseudo-population of the two comparison groups: n = 132.6 in the MRI (-) group and n = 83.1 in the MRI (+) group (Supplementary Table 3). Standardized mean differences in IPTW matching variables were < 0.11, except for one case (revision surgery) (Supplementary Table 4).

In the PS-matched and IPTW comparisons, operation time for FN identification in the MRI (+) group was significantly shorter than that in the MRI (-) group (P < 0.001) (Table 3). Conversely, operation time for FN dissection and tumor removal was not significantly different between the groups with and without MRI after PS matching or IPTW (Table 3).

Considering the mediating effect of surgical extent on FN outcomes, PS matching and stabilized IPTW methods revealed that temporary and permanent FNP rates were not significantly different between patients with and without 3D-DESS-WE-MRI (Table 4).

Table 2. Anatomical visibility of 3D-DESS-WE-MRI for parotid tumor location relative to the facial nerve (n = 120)

Surgical findings	MRI findings			
	Superficial	Deep	Both	Unknown (FN invisible)
Superficial	52	0	3	2
Deep	0	14	4	0
Both	1	0	43	1

3D-DESS-WE-MRI = three-dimensional double-echo steady-state water-excitation sequence magnetic resonance imaging, MRI = magnetic resonance imaging, FN = facial nerve

DISCUSSION

In our study, we confirmed an overall accuracy of 90.8% for the localization of parotid tumors relative to the FN, and a reduction in operation time for identification of the FN, with the use of preoperative 3D-DESS-WE-MRI. However, no statistically significant difference was found in FNP rates between patients with and without 3D-DESS-WE-MRI.

Previous studies have reported similarly high diagnostic accuracy (92%–97.8%) of 3D-DESS-WE-MRI in localizing parotid tumors [26,27]. MRI visibility of the FN in our

Table 3. Comparison of operation time in patients with vs. without preoperative FN imaging using 3D-DESS-WE-MRI

Method	Group	No.	Operation time #1			Operation time #2		
			Median (IQR), min	Coefficient estimate (95% CI)	P	Median (IQR), min	Coefficient estimate (95% CI)	P
Before PS matching	MRI (-)	165	30 (30.0 to 40.0)	Ref.		40.0 (30.0 to 45.0)	Ref.	
	MRI (+)	105	25.0 (25.0 to 30.0)	-0.28 (-0.35 to -0.21)	< 0.001	40.0 (35.0 to 55.0)	0.21 (0.14 to 0.29)	< 0.001
After PS matching	MRI (-)	65	35 (30.0 to 45.0)	Ref.		40.0 (30.0 to 50.0)	Ref.	
	MRI (+)	65	25 (25.0 to 30.0)	-0.51 (-0.52 to -0.49)	< 0.001	35.0 (35.0 to 50.0)	0.02 (-0.07 to 0.12)	0.653
Stabilized IPTW analysis	MRI (-)	133	30 (30.0 to 40.0)	Ref.		35.0 (30.0 to 45.0)	Ref.	
	MRI (+)	83	25 (25.0 to 30.0)	-0.28 (-0.35 to -0.21)	< 0.001	35.0 (35.0 to 50.0)	0.13 (-0.07 to 0.34)	0.207

Time to FN identification (operation time #1) and time to tumor removal (operation time #2) were transformed using natural log due to skewed distribution. Coefficient estimate (95% CI): Regression coefficient estimate, 95% confidence intervals (CIs). Statistical analysis using a generalized estimating equation (PS matching), or a logistic regression model with a stabilization (trimming) of extreme propensity scores (< 0.1 or > 0.9) (stabilized IPTW analysis).
FN = facial nerve, 3D-DESS-WE-MRI = three-dimensional double-echo steady-state water-excitation sequence magnetic resonance imaging, IQR = interquartile range, Ref. = reference, PS = propensity score, MRI = magnetic resonance imaging, IPTW = inverse probability of treatment weighting

https://doi.org/10.3348/kjr.2022.0850

Korean Journal of Radiology
KJR

Table 4. Comparison of FNP rates in patients with vs. without preoperative FN imaging using 3D-DESS-WE-MRI

Method	Group	No.	Temporary FNP			Permanent FNP		
			No. (%, 95% CI)	OR (95% CI)	*P*	No. (%, 95% CI)	OR (95% CI)	*P*
Before PS matching	MRI (-)	165	4 (2.4, 1.0 to 6.1)	Ref.		2 (1.2, 0.15 to 4.31)	Ref.	
	MRI (+)	105	26 (24.8, 17.5 to 33.8)	10.47 (3.80 to 36.96)	< 0.001	16 (15.2, 8.97 to 23.56)	11.03 (2.94 to 71.81)	< 0.001
After PS matching	MRI (-)	65	4 (6.2, 2.4 to 15.8)	Ref.		2 (3.1, 0.37 to 10.68)	Ref.	
	MRI (+)	65	10 (15.4, 7.6 to 26.5)	2.29 (0.64 to 8.25)	0.206	5 (7.7, 2.54 to 17.05)	2.02 (0.32 to 12.90)	0.46
Stabilized IPTW analysis	MRI (-)	133	7 (5.1, 2.14 to 10.54)	Ref.		1 (0.7, 0.02 to 4.12)	Ref.	
	MRI (+)	83	17 (19.3, 12.4 to 30.8)	1.76 (0.19 to 16.75)	0.526	11 (12.3, 6.81 to 22.48)	1.94 (0.20 to 18.49)	0.567

The extent of surgery can be changed by MRI findings. In statistical analyses, we adjusted this potential mediator effect of the surgical extent, to estimate the relative impact of 3D-DESS-WE-MRI on FNP occurrence. Statistical analysis using a generalized estimating equation (PS matching), or a logistic regression model with a stabilization (trimming) of extreme propensity scores (< 0.1 or > 0.9) (stabilized IPTW analysis).
FNP = facial nerve palsy, FN = facial nerve, 3D-DESS-WE-MRI = three-dimensional double-echo steady-state water-excitation sequence magnetic resonance imaging, CI = confidence interval, OR = odds ratio, PS = propensity score, MRI = magnetic resonance imaging, Ref. = reference, IPTW = inverse probability of treatment weighting

study (main trunk, 97.5%; temporofacial division, 42.5%; cervicofacial division, 25%) was slightly lower than in a previous report (main trunk, 100%; temporofacial division, 48%; cervicofacial division, 36%) [27]. In a study of 18 healthy volunteers, Qin et al. [22] reported higher visibility rates of the temporofacial and cervicofacial divisions (55.6% and 94.4%, respectively). Most of these differences appear to be attributed to different study participants (healthy volunteers versus patients with parotid tumors) [22].

In our study, we only included cases requiring FN identification and dissection. Nevertheless, distribution of variables between the groups with and without MRI was severely skewed, leaving more unfavorable cases of FNP in the MRI (+) group. This uneven distribution may be due to the surgeon's decision to preserve the FN during parotidectomy. If surgeons anticipated difficulties in preserving the FN, they tended to obtain more anatomical information before surgery with 3D-DESS-WE-MRI. To overcome the limitations of study design, we conducted PS matching and IPTW analyses to adjust for uneven distribution of risk variables and compare clinical outcomes. In addition to estimating the average effect of MRI intervention for the MRI (+) group through PS matching analysis, we also investigated the average effect of MRI intervention for the total enrolled patients with parotid tumors with IPTW analysis. For PS matching, we selected suitable variables for FNP among surgical and tumor factors. Tumor factors, such as tumor size, multiplicity, pathology, and location, were based on surgical findings; however, surgical extent largely depended on preoperative CT or MRI findings (tumor factors). We regarded surgical extent as having a mediator effect on FNP; therefore, this variable was excluded from PS matching. We also adjusted for the mediator effect of surgical extent in PS matching and IPTW comparisons. Similarly, clinical findings (mobility of tumors) were highly dependent on tumor size and location; therefore, we excluded these variables from the adjusted matching model.

An initial comparison (before PS matching) revealed higher incidence of FNP in the MRI (+) group. However, PS matching and IPTW analyses revealed that the occurrence of FNP was not significantly different between the two groups with or without MRI, suggesting a selection bias. In summary, FN outcomes in parotidectomy did not vary between patients with and without 3D-DESS-WE-MRI, although MRI preoperatively provided accurate anatomical information regarding the FN and tumor. Even with knowledge regarding FN and tumor location, functional

https://doi.org/10.3348/kjr.2022.0850

preservation of the FN seems to depend on the surgical technique, manipulation, and tumor characteristics (e.g., inflammation, fibrosis, adhesion, and status of tumor capsule) [2,3,6-11]. This study did not quantify surgical manipulation of the FN or surgical techniques; however, it is plausible that dissection, separation, and preservation of the FN from surrounding tissues or tumors require hard labor in large, deep-seated, and malignant tumors. Thus, we assumed that surgical manipulation of the FN around the tumor might be another (hidden) important factor for postoperative FN weakness, even in the risk-factor-adjusted comparison, despite using 3D-DESS-WE-MRI.

This assumption was also supported by our observation that operation time for FN identification was significantly shorter in the MRI (+) group than in the MRI (-) group; however, operation time for FN dissection and tumor removal was not. Thus, preoperative FN imaging with 3D-DESS-WE-MRI appears to play a role in localizing and identifying the FN during parotidectomy, rather than in functional preservation or dissection around tumors. Thus, anatomical information regarding the FN and tumors can help surgeons choose an adequate surgical approach, lower their distress regarding FN identification, and increase surgical confidence, even without an actual improvement in FN outcomes.

Our study had several limitations. First, we did not compare 3D-DESS-WE-MRI with conventional MRI; in the MRI (-) group, patients were evaluated only with CT scans. It is universally recognized that MRI is superior to CT in terms of tumor characterization [34-38]. However, our study focused on anatomically predicting the intra-parotid FN course using 3D-DESS-WE-MRI and determining clinical impact on parotid tumor surgery, rather than on tumor characterization. Second, this was a non-randomized study. To overcome this limitation, we conducted PS matching and IPTW to adjust for several variables. However, other factors that were not measured may have remained unadjusted between the two groups, which may have affected our conclusion. Finally, the low frequency of event (FNP) (2–4 in the MRI [-] group and 5–10 in the MRI [+] group) did not have enough statistical power. Thus, a larger prospective study with a randomized allocation to MRI intervention is needed to confirm our findings.

In conclusion, preoperative FN imaging with 3D-DESS-WE-MRI provides anatomical information about the FN and parotid tumors, and facilitates surgical identification of the FN during parotidectomy. While this reduced operation time for FN identification, it did not significantly affect postoperative FNP rate.

Supplement

The Supplement is available with this article at https://doi.org/10.3348/kjr.2022.0850.

Availability of Data and Material

All data generated or analyzed during the study are included in this published article and its supplementary information files.

Conflicts of Interest

The authors have no potential conflicts of interest to disclose.

Author Contributions

Conceptualization: Han-Sin Jeong, Yikyung Kim. Data curation: Hak Jung Kim, Eun-hye Kim. Formal analysis: Hyung-Jin Kim, Yikyung Kim, Sook-young Woo. Funding acquisition: Han-Sin Jeong. Investigation: Hak Jung Kim, Eun-hye Kim, Sook-young Woo. Methodology: Han-Sin Jeong, Yikyung Kim. Project administration: Han-Sin Jeong, Yikyung Kim. Resources: Hak Jung Kim, Eun-hye Kim. Supervision: Hyung-Jin Kim, Man Ki Chung, Young-Ik Son. Validation: Han-Sin Jeong, Yikyung Kim. Visualization: Han-Sin Jeong, Yikyung Kim. Writing—original draft: Han-Sin Jeong, Yikyung Kim. Writing—review & editing: Hyung-Jin Kim, Man Ki Chung, Young-Ik Son, Han-Sin Jeong.

ORCID IDs

Han-Sin Jeong
https://orcid.org/0000-0003-4652-0573
Yikyung Kim
https://orcid.org/0000-0002-9395-4879
Hyung-Jin Kim
https://orcid.org/0000-0003-3576-3625
Hak Jung Kim
https://orcid.org/0000-0001-9134-1430
Eun-hye Kim
https://orcid.org/0000-0001-7393-8671
Sook-young Woo
https://orcid.org/0000-0001-6577-3221
Man Ki Chung
https://orcid.org/0000-0002-1435-7786
Young-Ik Son
https://orcid.org/0000-0002-2114-8085

Korean Journal of Radiology
KJR

Funding Statement

This work was supported by grants from Samsung Medical Center (No. OTX0001031 and PHX0201451). The funders had no further role in study design; collection, analysis and interpretation of data; writing of the manuscript; or decision to submit this manuscript for publication.

REFERENCES

1. Bron LP, O'Brien CJ. Facial nerve function after parotidectomy. *Arch Otolaryngol Head Neck Surg* 1997;123:1091-1096
2. Guntinas-Lichius O, Gabriel B, Klussmann JP. Risk of facial palsy and severe Frey's syndrome after conservative parotidectomy for benign disease: analysis of 610 operations. *Acta Otolaryngol* 2006;126:1104-1109
3. Mehle ME, Kraus DH, Wood BG, Benninger MS, Eliachar I, Levine HL, et al. Facial nerve morbidity following parotid surgery for benign disease: the cleveland clinic foundation experience. *Laryngoscope* 1993;103(4 Pt 1):386-388
4. Mra Z, Komisar A, Blaugrund SM. Functional facial nerve weakness after surgery for benign parotid tumors: a multivariate statistical analysis. *Head Neck* 1993;15:147-152
5. Witt RL. Facial nerve function after partial superficial parotidectomy: an 11-year review (1987-1997). *Otolaryngol Head Neck Surg* 1999;121:210-213
6. Domenick NA, Johnson JT. Parotid tumor size predicts proximity to the facial nerve. *Laryngoscope* 2011;121:2366-2370
7. Jin H, Kim BY, Kim H, Lee E, Park W, Choi S, et al. Incidence of postoperative facial weakness in parotid tumor surgery: a tumor subsite analysis of 794 parotidectomies. *BMC Surg* 2019;19:199
8. Ikoma R, Ishitoya J, Sakuma Y, Hirama M, Shiono O, Komatsu M, et al. Temporary facial nerve dysfunction after parotidectomy correlates with tumor location. *Auris Nasus Larynx* 2014;41:479-484
9. Kadletz L, Grasl S, Grasl MC, Perisanidis C, Erovic BM. Extracapsular dissection versus superficial parotidectomy in benign parotid gland tumors: the Vienna Medical School experience. *Head Neck* 2017;39:356-360
10. Stathopoulos P, Igoumenakis D, Smith WP. Partial superficial, superficial, and total parotidectomy in the management of benign parotid gland tumors: a 10-year prospective study of 205 patients. *J Oral Maxillofac Surg* 2018;76:455-459
11. Yuan X, Gao Z, Jiang H, Yang H, Lv W, Wang Z, et al. Predictors of facial palsy after surgery for benign parotid disease: multivariate analysis of 626 operations. *Head Neck* 2009;31:1588-1592
12. Pather N, Osman M. Landmarks of the facial nerve: implications for parotidectomy. *Surg Radiol Anat* 2006;28:170-175
13. Rea PM, McGarry G, Shaw-Dunn J. The precision of four commonly used surgical landmarks for locating the facial nerve in anterograde parotidectomy in humans. *Ann Anat* 2010;192:27-32
14. Terrell JE, Kileny PR, Yian C, Esclamado RM, Bradford CR, Pillsbury MS, et al. Clinical outcome of continuous facial nerve monitoring during primary parotidectomy. *Arch Otolaryngol Head Neck Surg* 1997;123:1081-1087
15. Witt RL. Facial nerve monitoring in parotid surgery: the standard of care? *Otolaryngol Head Neck Surg* 1998;119:468-470
16. Eisele DW, Wang SJ, Orloff LA. Electrophysiologic facial nerve monitoring during parotidectomy. *Head Neck* 2010;32:399-405
17. Dulguerov P, Marchal F, Lehmann W. Postparotidectomy facial nerve paralysis: possible etiologic factors and results with routine facial nerve monitoring. *Laryngoscope* 1999;109:754-762
18. Sood AJ, Houlton JJ, Nguyen SA, Gillespie MB. Facial nerve monitoring during parotidectomy: a systematic review and meta-analysis. *Otolaryngol Head Neck Surg* 2015;152:631-637
19. Naganawa S, Ishihara S, Satake H, Kawai H, Sone M, Nakashima T. Simultaneous three-dimensional visualization of the intra-parotid facial nerve and parotid duct using a three-dimensional reversed FISP sequence with diffusion weighting. *Magn Reson Med Sci* 2010;9:153-158
20. Chu J, Zhou Z, Hong G, Guan J, Li S, Rao L, et al. High-resolution MRI of the intraparotid facial nerve based on a microsurface coil and a 3D reversed fast imaging with steady-state precession DWI sequence at 3T. *AJNR Am J Neuroradiol* 2013;34:1643-1648
21. Guenette JP, Ben-Shlomo N, Jayender J, Seethamraju RT, Kimbrell V, Tran NA, et al. MR imaging of the extracranial facial nerve with the CISS sequence. *AJNR Am J Neuroradiol* 2019;40:1954-1959
22. Qin Y, Zhang J, Li P, Wang Y. 3D double-echo steady-state with water excitation MR imaging of the intraparotid facial nerve at 1.5T: a pilot study. *AJNR Am J Neuroradiol* 2011;32:1167-1172
23. Al-Haj Husain A, Stadlinger B, Winklhofer S, Müller M, Piccirelli M, Valdec S. Mandibular third molar surgery: intraosseous localization of the inferior alveolar nerve using 3D double-echo steady-state MRI (3D-DESS). *Diagnostics (Basel)* 2021;11:1245
24. Al-Haj Husain A, Valdec S, Stadlinger B, Rücker M, Piccirelli M, Winklhofer S. Preoperative visualization of the lingual nerve by 3D double-echo steady-state MRI in surgical third molar extraction treatment. *Clin Oral Investig* 2022;26:2043-2053
25. Kwon D, Lee C, Chae Y, Kwon IJ, Kim SM, Lee JH. Clinical validation of the 3-dimensional double-echo steady-state with water excitation sequence of MR neurography for preoperative facial and lingual nerve identification. *Imaging Sci Dent* 2022;52:259-266
26. Fujii H, Fujita A, Kanazawa H, Sung E, Sakai O, Sugimoto H. Localization of parotid gland tumors in relation to the intraparotid facial nerve on 3D double-echo steady-state

with water excitation sequence. *AJNR Am J Neuroradiol* 2019;40:1037-1042
27. Kim Y, Jeong HS, Kim HJ, Seong M, Kim Y, Kim ST. Three-dimensional double-echo steady-state with water excitation magnetic resonance imaging to localize the intraparotid facial nerve in patients with deep-seated parotid tumors. *Neuroradiology* 2021;63:731-739
28. Austin PC. Balance diagnostics for comparing the distribution of baseline covariates between treatment groups in propensity-score matched samples. *Stat Med* 2009;28:3083-3107
29. Schacht A, Bogaerts K, Bluhmki E, Lesaffre E. A new nonparametric approach for baseline covariate adjustment for two-group comparative studies. *Biometrics* 2008;64:1110-1116
30. Xu S, Ross C, Raebel MA, Shetterly S, Blanchette C, Smith D. Use of stabilized inverse propensity scores as weights to directly estimate relative risk and its confidence intervals. *Value Health* 2010;13:273-277
31. Austin PC, Stuart EA. Moving towards best practice when using inverse probability of treatment weighting (IPTW) using the propensity score to estimate causal treatment effects in observational studies. *Stat Med* 2015;34:3661-3679
32. Lee BK, Lessler J, Stuart EA. Weight trimming and propensity score weighting. *PLoS One* 2011;6:e18174
33. Zeger SL, Liang KY, Albert PS. Models for longitudinal data: a generalized estimating equation approach. *Biometrics* 1988;44:1049-1060
34. Christe A, Waldherr C, Hallett R, Zbaeren P, Thoeny H. MR imaging of parotid tumors: typical lesion characteristics in MR imaging improve discrimination between benign and malignant disease. *AJNR Am J Neuroradiol* 2011;32:1202-1207
35. Habermann CR, Arndt C, Graessner J, Diestel L, Petersen KU, Reitmeier F, et al. Diffusion-weighted echo-planar MR imaging of primary parotid gland tumors: is a prediction of different histologic subtypes possible? *AJNR Am J Neuroradiol* 2009;30:591-596
36. Kei PL, Tan TY. CT "invisible" lesion of the major salivary glands a diagnostic pitfall of contrast-enhanced CT. *Clin Radiol* 2009;64:744-746
37. Lee YY, Wong KT, King AD, Ahuja AT. Imaging of salivary gland tumours. *Eur J Radiol* 2008;66:419-436
38. Yabuuchi H, Fukuya T, Tajima T, Hachitanda Y, Tomita K, Koga M. Salivary gland tumors: diagnostic value of gadolinium-enhanced dynamic MR imaging with histopathologic correlation. *Radiology* 2003;226:345-354

https://doi.org/10.3348/kjr.2022.0850